Molecular Catalysis 477 (2019) 110551

Contents lists available at ScienceDirect

Molecular Catalysis

journal homepage: www.elsevier.com/locate/mcat

Immobilized chiral rhodium nanoparticles stabilized by chiral P-ligands as efficient catalysts for the enantioselective hydrogenation of 1-phenyl-1,2-propanedione

Doris Ruiz[a,*], Päivi Mäki-Arvela[b], Atte Aho[b], Ricardo Chimentão[a], Carmen Claver[c], Cyril Godard[c], José L.G. Fierro[d], Dmitry Yu. Murzin[b]

[a] Physical Chemistry Department, Faculty of Chemistry, University of Concepcion, 407037, Concepcion, Chile
[b] Johan Gadolin Process Chemistry Centre, Åbo Akademi University, FI-20500 Turku/Åbo, Finland
[c] Departament de Química Física i Inorgànica, Facultat de Química, Universitat Rovira I Virgili, 43005 Tarragona, Spain
[d] Institute of Catalysis and Petrochemistry (CSIC), Cantoblanco, 28049, Madrid, Spain

ARTICLE INFO

Keywords:
Chiral nanoparticles
Rhodium
Enantioselective hydrogenation
Recyclable catalysts

ABSTRACT

This work reports the efficient synthesis of enantio-enriched alcohols by asymmetric hydrogenation of 1-phenyl-1,2-propanedione using chiral nanoparticles (NPs) supported on SiO_2. The chiral catalysts were synthesized by reducing the $[Rh(\mu-OCH_3)(C_8H_{12})]_2$ precursor under H_2 in the presence of P-chiral ligands as stabilizers and SiO_2 as support. Synthesis of catalysts in mild conditions was performed from labile organometallic precursor and chiral ligands provided small and well defined chiral nanoparticles ($\leq$ 3 nm). The catalysts were characterized by XPS, HR-TEM, EDS, XRD and N_2 physisorption isotherm. The physical chemical properties of the materials were correlated with the catalytic results obtained in the asymmetric hydrogenation of 1-phenyl-1,2-propanedione. In 1-phenyl-1,2-propanedione hydrogenation the best results using chiral catalysts allowed 98% conversion and enantiomeric excess of 67% to (*R*)-1-hydroxy-1-phenyl-propan-2-one and 59% for (*R*)-2-hydroxy-1-phenylpropan-1-one. Catalyst recycling studies revealed that chiral nanoparticles immobilized on SiO_2 are stable. These catalysts do not need extra amount of chiral modifier or inducer added *in situ* and could be reused without loss of enantioselectivity.

1. Introduction

Asymmetric synthesis by homogeneous and heterogeneous catalysis is commonly used for the production of optically pure chemicals for pharmaceuticals, flavoring and fragrances [1,2]. Specifically a considerable attention has been focused on the hydrogenation of α,β-unsaturated carbonyl compounds and α-ketoesters of high importance in the production of building blocks for fine chemicals industry [2,3]. One of the most studied α-ketoester, ethyl pyruvate, has been originally reported by Orito et al. [4,5] over cinchona alkaloid-modified platinum catalysts. Since then, a number of heterogeneous systems have been used in enantioselective hydrogenation [6–9]. High activity was reported in most cases, however a chiral inducer or modifier could be not recovered with the catalyst as it is added *in situ* and remains in the reaction media [10,11]. Otherwise, high activity and excellent selectivity obtained by a variety of homogeneous catalysts have been reported in asymmetric hydrogenations [12,13]. However, recent more stringent environmental requirements require clean technologies related to "green chemistry" principles such as milder operation conditions, high efficiency, reduction of emissions and mainly application of recyclable catalysts. It is, however, well known that homogeneous catalysts are difficult to recover from the reaction media [12].

Taking advantage of the high efficiency of catalysts [14] and ligands [15] used in homogeneous processes and feasibility of reusing heterogeneous catalysts, an increase in the synthetic scope of immobilization of these species has been widely studied in the last years [16]. In this field, chiral modification of metal surfaces has expanded successfully along the years [17–19]. A variety of experimental techniques provides chiral materials [20,21] including supported asymmetric homogeneous catalysts [20], chiral modifiers with heterogeneous supported metal catalysts [22–30], colloidal metal particles stabilized with chiral ligands [18,19,31–33], grafted chiral modifiers on supports [34–36], functionalized polymers [37] and chiral nanoparticles immobilized on metal oxide surfaces [20]. Typically SiO_2, Al_2O_3 or TiO_2 are the most

* Corresponding author.
E-mail address: doruiz@udec.cl (D. Ruiz).

https://doi.org/10.1016/j.mcat.2019.110551
Received 11 April 2019; Received in revised form 27 June 2019; Accepted 2 August 2019
Available online 24 August 2019
2468-8231/

used supports for this kind of heterogenization [20,36,38]. Contrary to polymeric matrices often used for anchoring ligands or organometallic complexes, mesoporous supports have the advantage of strong adsorption and good mechanical strength [20].

In the field of transition metal NPs, several methods of stabilization have been reported [39–46]. In the context of catalysis, control of size, shape and dispersion of metals on support surface is desirable due to their influence on the activity, selectivity and recycling [35,37]. This stabilization can be provided by traditional organic ligands [47–56] or polymers [38,57,58], and ionic liquids [59]. One of the simplest ways to incorporate organic compounds onto the surface is by adsorption which is possible through functional groups as phenyl rings or heteroatoms such as P or N [50,55,60,61].

The effect of ligand nature was elucidated in the enantioselective hydrogenation of 1-phenyl-1,2-propanedione (PPD) [19,22–31,33,34,63], which lead to an important intermediate in the synthesis of drugs [3]. Typically Pt was used as an active metal in enantioselective hydrogenation of PPD [19,22–35]. However, recently also other metals have been investigated in this reaction, such as Rh [19,63] and Ir [19,62]. Inspired by our previous results in enantioselective hydrogenation of PPD giving maximally 72% enantiomeric excess of (*R*)-1-hydroxy-1-phenylpropan-2-one at 57% conversion level at 25 °C under 40 bar hydrogen in cyclohexane as a solvent over Rh nanoparticles stabilized by chiral ligands and supported on SiO_2 [19], it was decided to test also other chiral ligands stabilizing Rh NPs. In the current work the synthesis of catalysts [18] allowed to obtain clean chiral-surfaces by reduction of an unsaturated metal precursor under mild conditions on SiO_2. The surface modification was performed by chiral ligands known as efficiently in asymmetric homogeneous catalysts. Chiral nanoparticles immobilized on SiO_2 were characterized by XPS, HR-TEM, EDS, XRD and N_2 physisorption and tested in hydrogenation of PPD.

2. Experimental

All experiments were carried out using standard Schlenk techniques and vacuum-lines. Substrates and solvents used in this study were analytical grade and treated by standard methods.

2.1. Materials

$RhCl_3{\cdot}3H_2O$ (38%), 1-phenyl-1,2-propanedione (99%), cis,cis-1,5-cyclooctadiene (≥ 95%), KOH (≥85%) and chiral ligands* were used as received from Aldrich without further purification.

Nomenclature used for chiral ligands*: DIPAMP, ≥95%; ((*S*,*S*)-1,2-bis[(2-methoxyphenyl)(phenylphosphino)]ethane), MANDYPHOS, ≥ 97%; ((1*R*,1′*R*′)-1,1′-bis(dicyclohexylphosphino)-2,2′-bis[(*R*)-(dimethylamino)phenylmethyl]ferrocene), BINAP; ((*R*)-(+)-2,2′-bis(diphenylphosphino)-1,1′-binaphthalene), (+)-DIOP, 98%; ((+)-2,3-*O*-Isopropylidene-2,3-dihydroxy-1,4-bis(diphenylphosphino)butane), (-)-DIOP, 98%; ((-)-2,3-*O*-Isopropylidene-2,3-dihydroxy-1,4-bis (diphenylphosphino)butane) and TANIAPHOS, ≥99%; ((R_P)-1-[(*R*)-α-(dimethylamino)-2-(diphenylphosphino)benzyl]-2-diphenylphosphino ferrocene).

The following chemicals, nn-pentane (99%), tetrahydrofuran (THF, 99.9%), allylmagnesium chloride (2 mol L^{-1} in THF), and dichloromethane (99.8%), all from Aldrich, and cyclohexane (99.5%), methanol (99.9%), diethylether (98%) and ethanol (96%), from Merck, were distilled prior reactions. Precursor and catalyst was prepared under purified N_2 atmosphere. N_2 and H_2 (99.995%) were purchased from Linde. SiO_2 was heated at 150 °C for 2 h before use to remove humidity.

2.2. Precursor synthesis

$Rh(\mu\text{-}Cl)(C_8H_{12})]_2$ was synthesized from $RhCl_3{\cdot}3H_2O$ (2.0 mmol) and 1.1 mL of cis, cis-1 5-cyclooctadiene in 20 mL of ethanol [18]. This solution was stirred under reflux at 70 °C for 3 h giving a yellow precipitate, which was filtered and washed with diethyl ether collecting 71% of yield. $[Rh(\mu\text{-}Cl)(C_8H_{12})]_2$ was obtained according to the following reaction:

$$2RhCl_3 + 2\,C_8H_{12} + 2CH_3CH_2OH \rightarrow [Rh(\mu\text{-}Cl)(C_8H_{12})]_2 + 4HCl + 2CH_3CHO \quad (1)$$

$[Rh(\mu-OCH_3)(C_8H_{12})]_2$ was prepared from $[Rh(\mu\text{-}Cl)(C_8H_{12})]_2$ (0.36 mmol) in dichloromethane (15 mL). This solution was added to KOH (0.71 mmol) in methanol (5 mL). Immediately a dark yellow solid, $[Rh(\mu-OCH_3)(C_8H_{12})]_2$, was obtained according to the following reaction:

$$[Rh(\mu\text{-}Cl)(C_8H_{12})]_2 + 2KOH + 2CH_3OH \rightarrow [Rh(\mu-OCH_3)(C_8H_{12})]_2 + 2KCl + 2H_2O \quad (2)$$

This solid was mixed with 10 mL of methanol and 15 mL of water. Then, the solution was filtered, washed and finally dried under vacuum without further purification allowing 75% of yield.

2.3. Catalysts synthesis

The catalysts synthesis was carried out following the procedure of two steps: Rh chiral nanoparticles synthesis and subsequent support immobilization. Unsupported and supported NPs catalysts were obtained from $[Rh(\mu-OCH_3)(C_8H_{12})]_2$ and stabilizers DIPAMP, (-)-DIOP, (+)-DIOP, TANIAPHOS, MANDYPHOS and BINAP as ligands to provide chiral surfaces.

Hydrogenation of a prochiral compound, PPD hydrogenation in Scheme 1, over catalysts synthesized from $[Rh(\mu-OCH_3)(C_8H_{12})]_2$ precursor and the chiral ligand (-)-DIOP was used to study the ligand effect on the catalysts synthesis.

Rh precursor and chiral ligands (DIPAMP, (-)-DIOP, (+)-DIOP, TANIAPHOS, MANDYPHOS and BINAP) with a Rh/Ligand mole ratio of 0.2 were dissolved in 80 mL of THF. For each rhodium precursor, the reductive treatment was carried out at 25 °C and 3 bar H_2 under

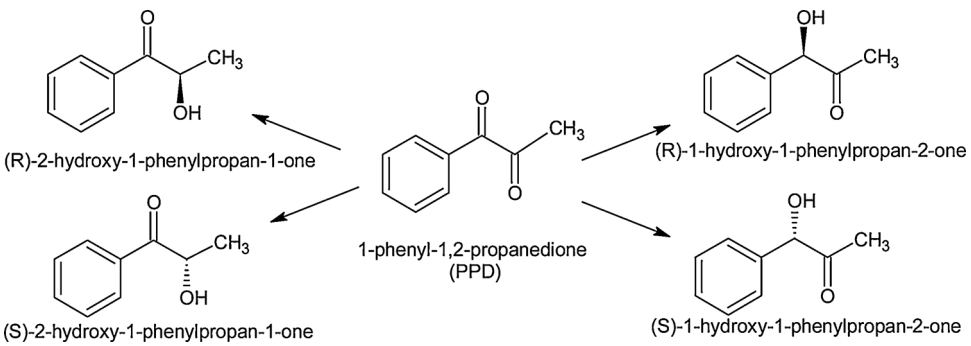

Scheme 1. Enantioselective hydrogenation of PPD.

Table 1
HR-TEM and textural characterization of Rh catalysts from $[Rh(\mu-OCH_3)(C_8H_{12})]_2$ precursor stabilized with chiral ligands.

Catalyst	d_{TEM} (nm)	D_{TEM}	S_{BET} (m^2/g)	d_{pore} (nm)	V_{pore} (cc/g)
Rh(-)-DIOP Nanoparticles	2.4 ± 1.1	–	–	–	–
Rh(-)-DIOP/SiO_2	2.4 ± 1.1	0.38	512	6.2	0.81
Rh-DIPAMP/SiO_2	1.8 ± 0.9	0.51	563	5.5	0.83
Rh-MANDYPHOS/SiO_2	2.4 ± 1.1	0.38	544	6.1	0.95
Rh-BINAP/SiO_2	2.5 ± 1.3	0.37	496	5.7	0.75
Rh-TANIAPHOS/SiO_2	2.0 ± 0.8	0.46	543	5.9	0.85
Rh(+)-DIOP/SiO_2	2.5 ± 1.1	0.37	583	5.4	0.85

d_{TEM} (metal diameter) and D_{TEM} (metal dispersion) determined by TEM.
S_{BET} (surface area), d_{pore} (pore diameter) and V_{pore} (pore volume) from Brunauer, Emmett and Teller (BET) and Barrett, Joyner and Halenda (BJH) models.

magnetic stirring for 40 h, 20 h and 70 h, respectively. Synthesis conditions of stabilized nanoparticles were previously optimized [18]. After synthesis, an appropriate amount of chiral nanoparticles was added onto dried SiO_2 obtaining 1 wt.% of Rh on SiO_2. 80 mL of THF was added to the mixture followed by stirring overnight at 25 °C. Finally, the chirally modified catalyst was washed with pentane (25 mL) and dried under vacuum for 3 h at 40 °C. Nomenclature used for catalysts is shown in Table 1.

The same procedure as mentioned above was also used for preparation of unsupported chiral nanoparticles (Rh_{free} NPs).

The ligand free 1 wt.% Rh/SiO_2 catalyst has been prepared from $[Rh(\mu-OCH_3)(C_8H_{12})]_2$ by the same procedure without, however, chiral ligands to assess if addition of ligands is beneficial for catalytic performance as such addition can be instrumental in regulating the growth of metallic clusters.

2.4. Catalysts characterization

Metal particle sizes were determined by transmission electron microscopy using a JEOL JEM-1011 equipment. Over 850 and 300 particles for NPs and supported catalysts, respectively, were analyzed. X-Ray Energy Dispersive Spectroscopy and Electron Diffraction were analyzed using this same equipment.

Nitrogen sorption isotherms at −196 °C were obtained with a Micromeritics ASAP 2010 (CHEMI) instrument. The samples (100 mg) were evacuated for 3 h at 150 °C before the surface area measurements. Brunauer, Emmett and Teller (BET) and Barrett, Joyner and Halenda (BJH) models were used to calculate the specific surface area, pore diameter and pore volume in all catalysts tested. The surface areas were calculated in the range of P/P° = 0.05-0.3.

XRD analyses was performed using a Rigatu New X-Ray "Geigerflex" D/max-IIC (40 Kv, 2 mA) diffractometer in the 2θ range of 10° to 90° (λ = 1.54056 Aº) at 1°/min.

Photoelectron spectra (XPS) were recorded using a Fisons Escalab 200R spectrometer equipped with a hemispherical analyzer using Mg K_α X-ray radiation ($h\nu$ = 1253.6 eV) at 10 mA and 12 kV.

The chemical structure of the synthesized precursor was confirmed by NMR ^1H in a Varian-Mercury 400 MHz equipment.

2.5. Hydrogenation reactions

Reactions were performed at 40 bar of H_2 pressure, 25 °C and stirring speed of 800 rpm to avoid external mass transfer limitations. Supported and unsupported NPs were tested as catalysts in hydrogenation reactions with a [substrate/metal] molar ratio of 100 in 50 mL of cyclohexane as a solvent. A stainless steel semibatch reactor coated with teflon was used for PPD enantioselective hydrogenation. In the preliminary experiments, different amounts of catalyst were used to investigate a potential impact of gas-liquid mass transfer and the results revealed that there were no gas-liquid mass transfer limitations. The catalyst particles were below 150 μm to suppress the internal mass transfer limitations.

The same conditions were used for the recycling tests, where Rh (-)-DIOP/SiO_2 catalyst was recycled by filtering and washing two times with n-pentane (15 mL) to remove compounds from the previous experiment. After treatment for 8 h in vacuum at 50 °C, the dried catalysts were used in the above mentioned conditions. Hydrogenation reaction over Rh_{free} NPs was performed using the same amount of Rh used with supported NPs catalysts.

The samples withdrawn from the reactor at different time intervals were analyzed using a SHIMADZU QP5050 GC–MS equipped with a chiral column β-DEX 225 (length 30 m, diameter 0.25 mm). The chromatographic program was generated by heating at 1 °C min^{-1} from 170 to 180 °C, with the column pressure of 90 kPa, column flow of 0.9 mL min^{-1}, total flow of 30.7 mL min^{-1} and the split ratio equal to of 20. Under these conditions, PPD and its hydrogenation products were identified by comparing their retention times with those of standards. Moreover, the structure of all compounds was verified by their mass spectra using GC–MS and the corresponding database. The retention times for substrate 1-phenyl-1,2-propanedione was 3.787 min, while for the reaction products they were 4.68; 4.93; 4.26 and 4.37 min, for *(R)*-1-hydroxy-1-phenylpropan-2-one, *(S)*-1-hydroxy-1-phenylpropan-2-one, *(S)*-2-hydroxy-1-phenylpropan-1-one and *(R)*-2-hydroxy-1-phenylpropan-1-one, respectively.

Activity was analyzed in terms of conversion, defined as $(c_{0,A}\text{-}c_A)/c_{0,A}$*100%, where $c_{0,A}$ and c_A denote the initial reactant concentration and the concentration of A at time t, respectively. The sum of the concentrations of reactant and products visible in GC analysis has been calculated as a function of time and denoted as GCLPA.

The initial TOF was calculated after 10 min of reaction time by dividing the converted moles of reactant by moles of the metal.

Enantiomeric excess was determined for PPD hydrogenation as

$$ee = ([R]\text{-}[S])/([R]+[S])x100\% \quad (3)$$

In PPD hydrogenation (Scheme 1), ee_1 and ee_2 are referred to *(R)-over the (S)*-enantiomer of 1-hydroxy-1-phenylpropan-2-one and 2-hydroxy-1-phenylpropan-1-one, respectively.

Regioselectivity (rs) is defined as the ratio between the concentrations of ($[R_1]$ + $[S_1]$) enantiomers obtained from hydrogenation of carbonyl-1 group and ($[R_2]$ + $[S_2]$) enantiomers formed from carbonyl-2 hydrogenation as

$$rs = [R_1]+[S_1])/([R_2]+[S_2]) \quad (4)$$

3. Results and discussion

3.1. Catalysts characterization

The textural parameters of supported and unsupported NP_S from $[Rh(\mu-OCH_3)(C_8H_{12})]_2$ precursor [18,64,65] are shown in Table 1. HR-TEM results revealed that all catalysts from NPs with ligands exhibited smaller metal particle sizes (< 3 nm), compared to ligand free NPs and 1 wt.% Rh/SiO_2 catalyst (both *ca.* 5.1 nm).

H_2 as a reducing agent under mild conditions generates highly reproducible particle sizes from $[Rh(\mu-OCH_3)(C_8H_{12})]_2$ releasing CH_3OH and inert C_8H_{16} species from their hydrogenation. Specifically, a small metal size is directly related to the presence of chiral ligands in the synthesis of nanoparticles during the metal precursor reduction. Fig. 1 displays a comparison of unsupported and supported, nanoparticles stabilized with (-)-DIOP.

Table 1 shows HR-TEM results for supported particles from $[Rh(\mu-OCH_3)(C_8H_{12})]_2$ and different chiral ligands confirming minor changes in metal dispersion up to 51% and diameters ≤ 2.5 nm. BINAP, DIPAMP, TANIAPHOS, MANDYPHOS, (+)-DIOP and (-)-DIOP ligands

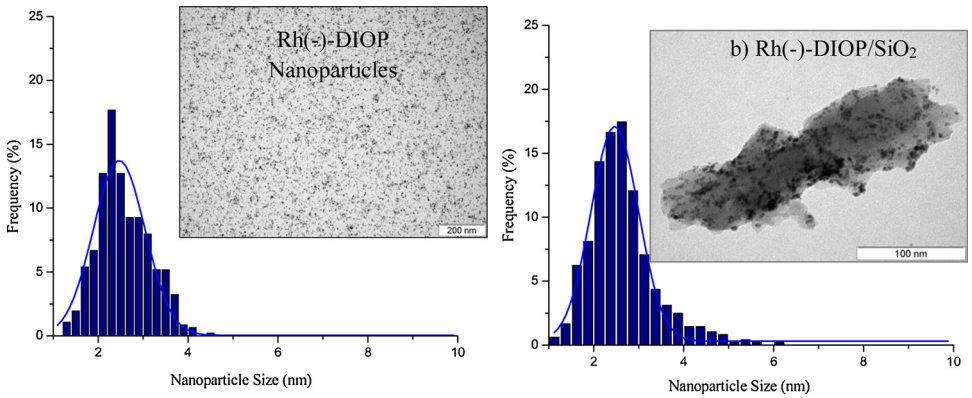

Fig. 1. Electron micrographs and size distribution of a) unsupported Rh Chiral NPs and b) 1 wt.% Rh/SiO_2 chiral catalyst from $[Rh(\mu-OCH_3)(C_8H_{12})]_2$ precursor.

(Fig. 2) allow to control the metal agglomeration and provide chiral surfaces. For this kind of systems it has been reported that stabilization occurs by adsorption of phenyl rings or heteroatoms as P or N (such as those present in Fig. 2) on the metal surface [50].

BET specific surface areas vary between 496 and 583 $m^2 g^{-1}$ and the isotherms correspond to type IV (IUPAC classification). The specific surface are of the neat SiO_2 support was 550 $m^2 g^{-1}$. This value in comparison with the value of supported metals illustrate that introduction of the metals did not result in significant alterations of the surface area.

A low metal content and small metal particle sizes were also verified by XRD which did not show any signals for Rh. A broad peak between 15 and 35° with a maximum at 2θ = 22.0° corresponding to SiO_2 was present in all catalysts.

Electron diffraction allowed verifying reduced rhodium species and interplanar spacing of $d_{hkl} = 2.1658$ Å. By X-Ray Energy Dispersive Spectroscopy was possible to identify Rh and SiO_2.

The degree of reduction and the surface composition were established by XPS. Table 2 summarizes atomic percentages and atomic surface ratios of Rh catalysts. The catalyst from chiral stabilized NPs showed a high content of Rh on the surface. A high percentage of reduced Rh was obtained without any reduction pretreatment. XPS analysis confirmed that a small flow or stream in H_2 allows reduction of rhodium species on the catalyst surface, therefore a conventional reduction procedure at a high temperature prior to each reaction is not necessary using these catalysts. The reason for such behavior is that ligands or organic compounds acting as stabilizers for metal surface generally prevent metal oxidation [20,50].

Binding energies of O1s and Si2p core-levels appeared at 532.6 and 103.4 eV, respectively. All catalysts showed binding energies centered at 307.0 and 309.0 eV for $Rh3d_{5/2}$ core level corresponding to both Rh^0 and $Rh^{\delta+}$, respectively (Fig. 3). Only for unsupported NPs and Rh-DIPAMP/SiO_2 catalysts it was possible to determine phosphorus BE P2p on the surface at 133.1 eV, confirming the presence of ligands on the surface. In other supported nanoparticles it was not possible to detect heteroatoms due to a high amount of SiO_2 (99 wt.%) and Rh immobilization occurring preferably inside the bulk support, which is in agreement with nitrogen physisorption (Table 1). Rh-DIPAMP on surface could be explained by the presence of methoxy substituents in the structure of the chiral ligand interacting with the Si−OH groups on the surface.

The characterization results reported in this work showed that synthesis of catalysts from $[Rh(\mu-OCH_3)(C_8H_{12})]_2$ in the presence of chiral ligand (-)-DIOP is very reproducible. Regarding the use of chiral ligands, (-)-DIOP, DIPAMP and BINAP showed the highest Rh/Si ratio on the surface (Table 2). Differences in the ratio of metal on surface found are associated with the stabilizer ligand nature and therefore its interaction with the surface during the synthesis of metal clusters.

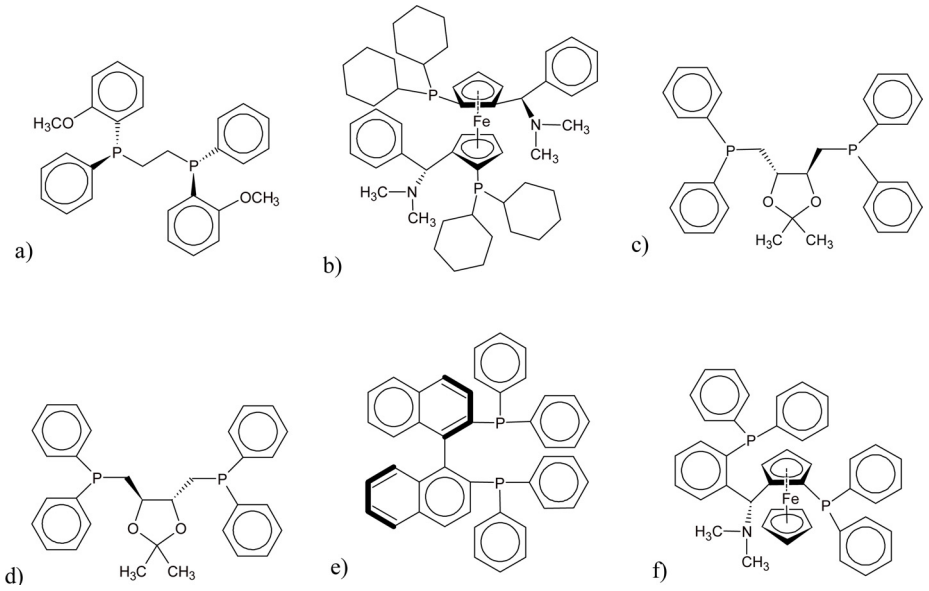

Fig. 2. Chiral ligands: a) DIPAMP, b) MANDYPHOS, c) (+)-DIOP, d) (-)-DIOP, e) BINAP and f) TANIAPHOS.

Table 2
Binding energies of core levels and atomic surface ratio of Rh catalysts.

Catalyst	Rh $3d_{5/2}$ (eV)	P 2p (eV)	P at, %	Rh at, %	Rh/P at ratio	Rh/Si at ratio
Rh(-)-DIOP Nanoparticles	307.1 (76); 309.2 (24)	133.0	8.3	7.2	0.9	–
Rh(-)-DIOP/SiO_2	307.1 (80); 309.0 (20)	–	–	0.9	–	0.030
Rh-TANIAPHOS/SiO_2	307.0 (84); 309.0 (16)	–	–	0.5	–	0.012
Rh-DIPAMP/SiO_2	307.1 (87); 309.0 (13)	133.0	–	0.9		0.042
Rh-MANDYPHOS/SiO_2	307.1 (87); 309.0 (13)	–	–	0.4	–	0.013
Rh-BINAP/SiO_2	307.1 (74); 308.8 (26)	–	–	0.9	–	0.030
Rh(+)-DIOP/SiO_2	307.0 (84); 309.0 (16)	–	–	0.3	–	0.006

3.2. PPD hydrogenation

Supported Rh NPs stabilized by ligands were studied as chiral catalysts in the PPD enantioselective reaction (Scheme 1). PPD is a very important substrate and the main product in its hydrogenation, (*R*)-1-hydroxy-1-phenylpropan-2-one acts as an intermediate for production of L-ephedrine [66]. Many compounds can be obtained from hydrogenation of PPD as reported in the literature [3,22–31] presenting also the values of rate constants.

The initial TOFs obtained for PPD hydrogenation using supported Rh NPs stabilized by different ligands (Table 3) diminished in the following order: Rh(-)-DIOP/SiO_2 > Rh(+)-DIOP/SiO_2 > Rh-TANIAPHOS/SiO_2 = Rh-MANDYPHOS/SiO_2 > > Rh-DIPAMP/SiO_2. This tendency is not directly correlated with the metal dispersion or the amount of metal on the surface (Table 1, Table 2). For Rh-BINAP/SiO_2 the initial TOF after 10 min was not calculated due to an induction time of 20 min (Fig. 4). Thereafter PPD disappeared nearly completely from the liquid phase due to strong interactions with the catalyst. This catalyst contained also the lowest amount of metallic Rh (Table 3). On the other hand, even if Rh-DIPAMP/SiO_2 exhibited the smallest metal size and also more ligand on the surface confirmed by XPS (P 2p at 133 eV) compared to the other catalysts, it gave the lowest initial TOF.

Conversion of PPD decreased in the following order: Rh-BINAP/SiO_2 > Rh(-)-DIOP nanoparticles > Rh(-)-DIOP/SiO_2 (Fig. 4). Rh-BINAP/SiO_2 gave also the lowest GCLPA (defined as the sum of concentrations of reactant and products visible in GC analysis), which is in accordance with XPS results showing that a large amount of ligand is present on the surface (Table 2). Low GCLPA levels were obtained both for Rh-(-)DIOP nanoparticles and for Rh-(-)DIOP/SiO_2 and the highest values were determined for Rh-TANIAPHOS/SiO_2 and for MANDYPHOS/SiO_2, which did not contain any oxygenated functional groups, but instead dimethyl amine functionality. The low GCLPA is due to strong adsorption of PPD or products on the catalyst surface. Interestingly, it was observed in catalyst recycling that the GCLPA levels increased indicating some changes in the ligand, although the enantiomeric excess was retained (See Catalyst Recycling section).

The kinetic profiles for PPD hydrogenation over different catalysts are shown in Figs. 5–9 and discussed for each catalyst separately. Thereafter, the yield of the desired product (*R*)-1-hydroxy-1-phenylpropan-2-one was correlated with the metal particles size.

The kinetic data for PPD hydrogenation over Rh-(-)-DIOP nanoparticles (Fig. 5a) showed that the transformation of PPD is initially rather fast during the first 100 min. The total concentration (i.e. sum of the reactant and product concentrations visible in GC analysis) declines also 150 fold more rapidly during first 30 min than during 30–220 min of the reaction (Fig. 5a). Thereafter the GCLPA declined even more slowly. This result indicates that the reactant and products are strongly adsorbed on the surface of catalyst particles. The maximum yield of the main product, (*R*)-1-hydroxy-1-phenylpropan-2-one is ca. 17% at 150 min, after which its concentration declined, while the concentration of S-enantiomer is increasing with increasing time. Interestingly GCLPA remains stable after 240 min. The ee_1 increased more rapidly than ee_2 at high conversion levels (Fig. 5b) although no diols are formed. This indicates that further transformations of R-enantiomer giving oligomers there was an increase in the enantiomeric excess, ee_1 with conversion. (*R*)-1-hydroxy-1-phenylpropan-2-one is thus more reactive than the corresponding S-enantiomer in such reactions leading to catalyst deactivation. The formed adsorbed species or oligomers could not be identified by GC analysis.

The regioselectivity also declined with increasing conversion

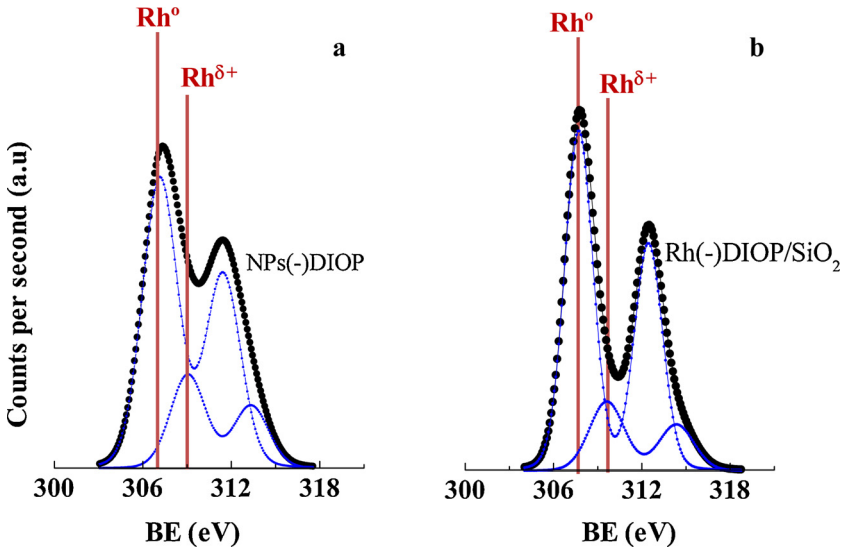

Fig. 3. Binding energies (eV) of internal levels of a) unsupported Rh NPs and b) supported catalysts prepared from $[Rh(\mu-OCH_3)(C_8H_{12})]_2$ precursor.

Table 3
Initial turn over frequency (TOF) (ee_1, ee_2 and rs at 70% conversion level for PPD hydrogenation over supported NPs obtained by stabilization with chiral ligands. Reaction conditions: PPD concentration 0.02 mol L^{-1}, (PPD/Rh) molar ratio: 100, 25 °C, 40 bar H_2, stirring rate: 800 rpm, solvent: 50 mL of cyclohexane.

Catalyst[a]	TOF[b] (s^{-1})	Conv.[c] (%)	GCLPA[c] (%)	Yield of R-1 (%)[d]	ee_1[d] (%)	ee_2[d] (%)	rs[d]
Rh(-)-DIOP nanoparticles		97	16	10	43	56	2
Rh(-)-DIOP/SiO_2	0.038	96	23	23	48	42	4
Rh(+)-DIOP/SiO_2	0.034	90	55	23	44	62	2
Rh-TANIAPHOS/SiO_2	0.016	72[e]	75[e]	37	40	68	14
Rh-DIPAMP/SiO_2	0.0033	80	35	13	40	62	12
Rh-MANDYPHOS/SiO_2	0.016	90	50	25	29	58	19

[a] 1 wt.% Rh-Ligand/SiO_2 catalysts from $[Rh(\mu-OCH_3)(C_8H_{12})]_2$ precursor.
[b] initial TOF during the first 10 min, calculated as mole converted per mole Rh in second.
[c] Conversion and GCLPA at 300 min of reaction.
[d] at 70% conversion.
[e] at 230 min.

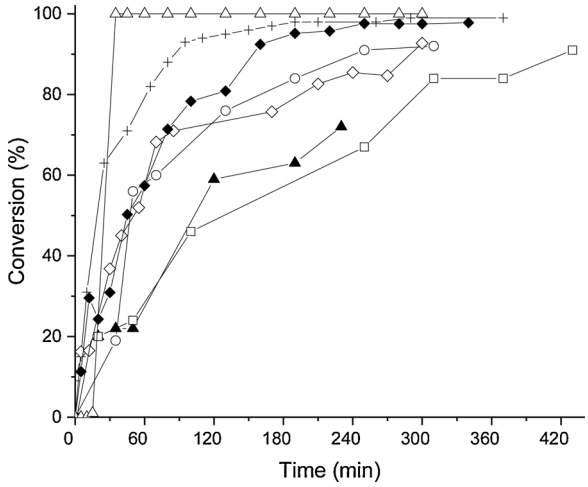

Fig. 4. Evolution of PPD conversion with reaction time for catalysts synthesized from $[Rh(\mu-OCH_3)(C_8H_{12})]_2$ with different ligands. Reaction conditions: PPD concentration 0.02 mol L^{-1}, molar ratio PPD/Rh: 100/1, stirring rate: 800 rpm, 25 °C, 40 bar H_2, solvent: 50 mL of cyclohexane. Notation: Rh-(-)-DIOP nanoparticles (+), Rh-(-)-DIOP/SiO_2 (♦), Rh-(+)-DIOP/SiO_2 (◊), Rh-BINAP/SiO_2 (Δ), Rh-TANIAPHOS/SiO_2 (▲), Rh-DIPAMP/SiO_2 (□) and Rh-MANDYPHOS/SiO_2 (o).

(Fig. 5b). The preferred carbonyl to be hydrogenated was the adjacent to the phenyl group in PPD as reported in [28]. The reason for the high regioselectivity towards hydrogenation, especially at the beginning of the experiment is that C=O (1) is in the same plane as the phenyl ring. Furthermore, it has been shown by quantum chemical calculations using B3LYP, HF and MP2 methods that the C=O bond at C1 is weaker than at C2. At high conversion levels when the concentration of PPD is low, there are more chances for PPD adsorption by C=O (2) [28].

For Rh-(+)-DIOP/SiO_2 the kinetic profiles are shown in Fig. 6. Interestingly, in this case the GCLPA remained quite high, being 55% after 300 min, while for Rh(-)-DIOP/SiO_2 it was much lower. This result indicates that chirality of the ligand has an effect on GCLPA and on the interactions of the reactant and products with the surface. The yield of the main product, (*R*)-1-hydroxy-1-phenylpropan-2-one (Fig. 6a) was also rather high, 30% at 240 min and its concentration profile remained relatively constant after 70 min opposite to Rh-(-)DIOP/SiO_2. Enantioselectivity ee_1 increased with conversion, while ee_2 was not increasing after prolonged times (Fig. 6b). Regioselectivity exhibited a similar declining trend as for Rh(-)DIOP/SiO_2, although being only half the one obtained by Rh(-)-DIOP/SiO_2 (Table 3). This is due to the high concentration of (*R*)-1-hydroxy-1-phenylpropan-2-one even at the end of the experiment opposite to the case for Rh-(-)-DIOP/SiO_2. The main difference between these two catalysts was that Rh(-)DIOP/SiO_2 exhibited 3 fold more Rh on its surface in comparison to Rh(+)DIOP/SiO_2 (Table 2).

For Rh-DIPAMP/SiO_2 an induction period can be seen in Fig. 7a. Finally, this catalyst provided the second lowest conversion of PPD after 300 min after Rh-TANIAPHOS/SiO_2 (Table 3) despite its high metal dispersion. The ee values were, however, with Rh-DIPAMP/SiO_2 on the same level (Fig. 6b) as for Rh-TANIAPHOS/SiO_2 (Table 3). It should be pointed out here, that the yield of the desired product is even more important than ee, especially for the cases where reaction proceeded slowly, e.g. Rh-DIPAMP/SiO_2 and thus an overall comparison of the yield of (*R*)-1-hydroxy-1-phenylpropan-2-one as a function of metal particle size is presented at the end of this section.

The GCLPA levels were very high for the two ligand-modified supported Rh catalysts containing dimethylamine group, namely Rh-MANDYPHOS/SiO_2 and Rh-TANIAPHOS/SiO_2 (Fig. 8 and 9). Both of these ligands contain not only amino groups, but also metallocene

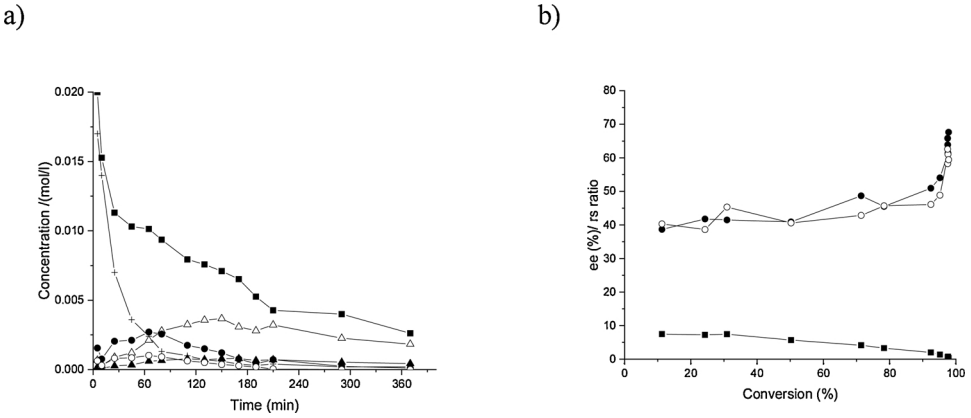

Fig. 5. a) Evolution of PPD and products concentration (Notation: Sum of concentrations (■), PPD (+), (*R*)-1-hydroxy-1-phenylpropan-2-one (▲) and (*S*)-2-hydroxy-1-phenylpropan-1-one (o), (*R*)-1-hydroxy-1-phenylpropan-2-one (▲) and (*S*)-2-hydroxy-1-phenylpropan-1-one (Δ) with reaction time and b) ee_1 (●) ee_2 (o) and regioselectivity (■) as a function of conversion over Rh(-)-DIOP nanoparticles. Reaction conditions: PPD concentration 0.02 mol L^{-1}, molar ratio (PPD/Rh): 100, stirring rate: 800 rpm, 25 °C, 40 bar H_2, solvent: 50 mL of cyclohexane.

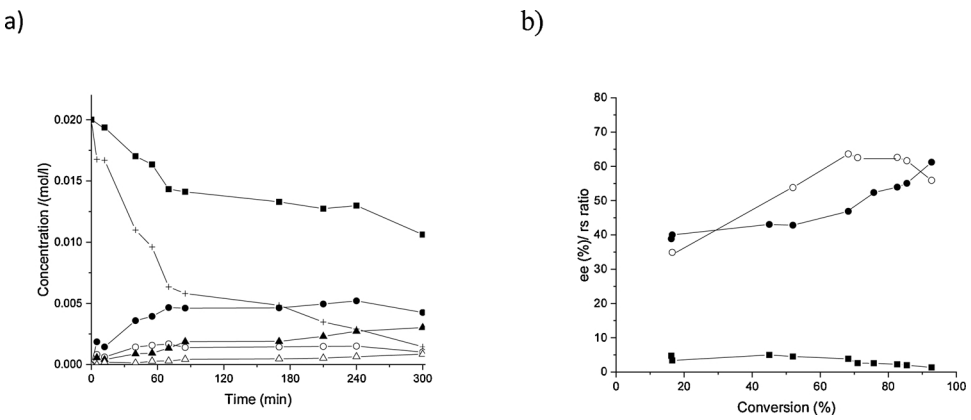

Fig. 6. a) Evolution of PPD and products concentration (Notation: Sum of concentrations (■), PPD (+), (*R*)-1-hydroxy-1-phenylpropan-2-one (●) and (*S*)-2-hydroxy-1-phenylpropan-1-one (o), (*R*)-2-hydroxy-1-phenylpropan-1-one (▲) and (*S*)-2-hydroxy-1-phenylpropan-1-one (Δ) with reaction time and b) ee_1 (●) ee_2 (o) and regioselectivity (■) as a function of conversion over Rh(+)-DIOP/SiO_2. Reaction conditions: PPD concentration 0.02 mol L^{-1}, molar ratio (PPD/Rh): 100, stirring rate: 800 rpm, 25 °C, 40 bar H_2, solvent: 50 mL of cyclohexane.

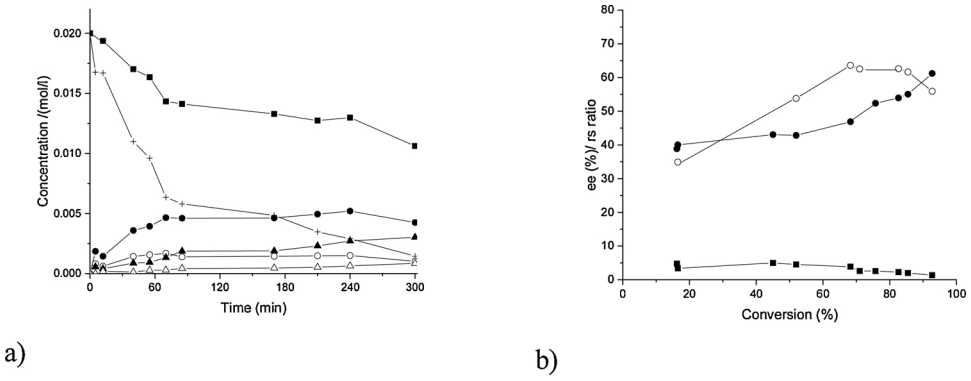

Fig. 7. a) Evolution of PPD and products concentration (Notation: Sum of concentrations (■), PPD (+), (*R*)-1-hydroxy-1-phenylpropan-2-one (●), (*S*)-1-hydroxy-1-phenylpropan-2-one (o), (*R*)-2-hydroxy-1-phenylpropan-1-one (▲) and (*S*)-2-hydroxy-1-phenylpropan-1-one (Δ) with reaction time and b) ee_1 (●) ee_2 (o) and regioselectivity (■) as a function of conversion over Rh-DIPAMP/SiO_2. Reaction conditions: PPD concentration 0.02 mol L^{-1}, molar ratio (PPD/Rh): 100, stirring rate: 800 rpm, 25 °C, 40 bar H_2, solvent: 50 mL of cyclohexane.

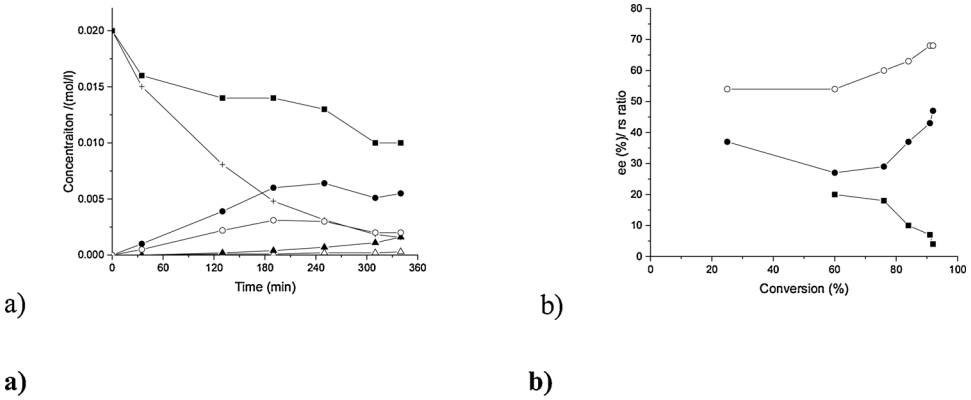

Fig. 8. a) Evolution of PPD and products concentration (Notation: Sum of concentrations (■), PPD (+), (*R*)-1-hydroxy-1-phenylpropan-2-one (●) and (*S*)-1-hydroxy-1-phenylpropan-2-one (o), (*R*)-2-hydroxy-1-phenylpropan-1-one (▲) and (*S*)-2-hydroxy-1-phenylpropan-1-one (Δ) with reaction time and b) ee_1 (●) ee_2 (o) and regioselectivity (■) as a function of conversion over Rh(+)-MANDYPHOS/SiO_2. Reaction conditions: PPD concentration 0.02 mol L^{-1}, molar ratio (PPD/Rh): 100, stirring rate: 800 rpm, 25 °C, 40 bar H_2, solvent: 50 mL of cyclohexane.

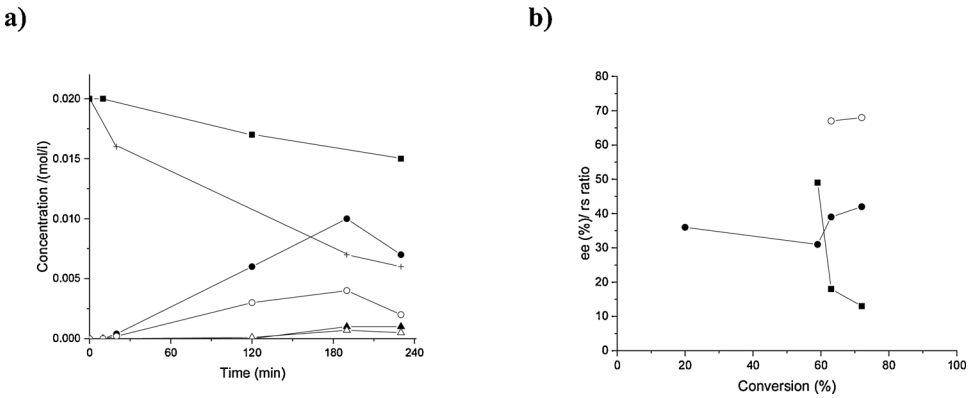

Fig. 9. Evolution of PPD and products concentration (Notation: Sum of concentrations (■), PPD (+), (*R*)-1-hydroxy-1-phenylpropan-2-one (●), (*S*)-1-hydroxy-1-phenylpropan-2-one (o), (*R*)-2-hydroxy-1-phenylpropan-1-one (▲) and (*S*)-2-hydroxy-1-phenylpropan-1-one (Δ) with reaction time and b) ee_1 (●) ee_2 (o) and regioselectivity (■) as a function of conversion over Rh-TANIAPHOS/SiO_2. Reaction conditions: PPD concentration 0.02 mol L^{-1}, molar ratio (PPD/Rh): 100, stirring rate: 800 rpm, 25 °C, 40 bar H_2, solvent: 50 mL of cyclohexane.

(ferrocene), which could decrease interactions with PPD and its products.

Over Rh-(+)MANDYPHOS/SiO_2 and Rh-TANIAPHOS/SiO_2 the maximum yields of (*R*)-1-hydroxy-1-phenylpropan-2-one were 30% and 50% at 240 min and 182 min, respectively (Fig. 8a, 9 a). Enantiomeric excesses for the main product, i.e. ee_1 were about at the same level as for Rh-(-)DIOP/SiO_2, while regioselectivities for Rh-MANDYPHOS/SiO_2 and Rh-DIPAMP/SiO_2 were much higher being 19 and 12 at 70% conversion than obtained for Rh-(-)DIOP/SiO_2 (Table 3). This result clearly shows also that the ligand structure has an

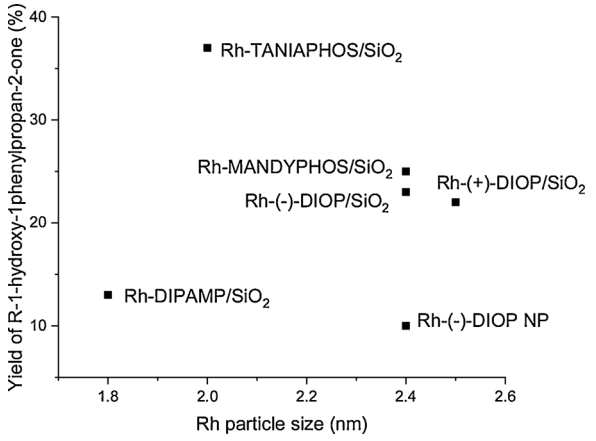

Fig. 10. The average Rh particle size as a function of the yield of the main product, (*R*)-1-hydroxy-1-phenylpropan-2-one at 70% conversion.

effect on product distribution. High regioselectivity obtained over Rh-MANDYPHOS/SiO_2 and Rh-DIPAMP/SiO_2 indicates that it is more challenging for C = O at position C2 to be in contact with Rh.

The highest yield of the desired product was obtained with Rh-TANIAPHOS/SiO_2 exhibiting an optimum metal particle size of 2 nm (Table 1), while e.g. Rh-DIPAMP/SiO_2 with a smaller metal particle size gave only 13% yield of the desired product (Fig. 10). In enantioselective hydrogenation of (-)-cinchonidine modified Pt catalyst, in which an optimum Pt particle size facilitated simultaneous adsorption and interaction of the modifier and the reactant on metal surface, being, however, slightly larger than in the current case, i.e. 3.8 nm for Pt/SiO_2 [30]. The correlation with the fraction of Rh^0 in XPS results (Table 2) shows also that the lowest yield of (*R*)-1-hydroxy-1-phenylpropan-2-one at 70% conversion, i.e. 10%, was obtained with Rh-(-)DIOP nanoparticles exhibiting only 76% of Rh in metallic state, whereas Rh/TANIAPHOS/SiO_2 with 80% Rh^0 gave 37% yield.

When comparing the current results obtained by Rh-DIPAMP/SiO_2, R-TANIAPHOS/SiO_2 and Rh(-)-DIOP/SiO_2 with those reported in the literature for PPD hydrogenation (Table 4), it can be observed that the ee_1 values obtained for ligand-Rh/SiO_2 are rather high. The metal particle sizes in ligand-Rh/SiO_2 are small in comparison with the case, in which (-)-cinchonidine was used as a modifier with Pt supported catalysts, since cinchonidine adsorption requires a relatively large metal particle. A small Rh particle size is an advantage helping to utilize the metal surface. One of the main benefits with these ligand-Rh/SiO_2 catalysts is that only mild conditions are required to reduce the metal nanoparticle in the presence of ligand opposite to conventional Pt supported catalysts, which should be reduced prior to the reaction at high temperature [22–30].

3.3. Catalyst recycling

One of the main objectives of this work was to study the reusability of chiral Rh(-)-DIOP/SiO_2 catalysts in PPD hydrogenation. The spent catalyst was washed between the experiments with pentane and dried in vacuum. The performance of the fresh and reused supported Rh (-)-DIOP/SiO_2 was compared with that of the unsupported Rh(-)-DIOP nanoparticles (Table 5). It can be observed that the highest initial transformation rate of PPD as well as the final conversion were obtained for Rh-(-)-DIOP nanoparticles followed by fresh Rh-(-)-DIOP/SiO_2, once used and twice used and the GCLPA was inversely proportional to the conversion level (Fig. 11a). The GCLPA indicates that the interactions of the reactant and/ or products are the most prominent with Rh-(-)-DIOP nanoparticles and less prominent for the reused catalysts. The reused catalyst exhibited a lower reaction rate, but no clear deactivation was observed and the final conversion with this catalyst was 88%. The catalyst reused twice showed an analogous kinetic profile as the once reused catalyst giving the conversion level of 76%. The reason for the lower conversion levels obtained with the reused Rh (-)-DIOP/SiO_2 is a slight increase in the average Rh particle sizes, confirmed by TEM analysis, as it was performed for the catalysts after the reaction. The average Rh particle sizes for fresh, once used and twice reused were 2.4, 2.9 and 3.2 nm, respectively.

The enantiomeric excess, on the other hand is slightly increasing with recycling (Table 5, Fig. 11b). Interestingly the highest regioselectivity was determined for once reused catalysts (Fig. 11b). These results are promising, clearly showing that chirality is retained in the reused catalysts.

4. Conclusions

Chiral metal supported catalysts stabilized by P-ligands have shown promising behavior as heterogeneous catalysts for the enantioselective hydrogenation of 1-phenyl-1,2-propanedione. Reduction of organometallic Rh precursor in the presence of ligands under mild conditions allowed to obtain clean chiral Rh surfaces that can be used more than once without additional amounts of chiral inducer *in situ*. Differences in activity and enantioselectivity have been discussed according to catalytic properties and characterization data, obtained with XPS and HR-TEM. An optimum Rh particle size of 2 nm over Rh-TANIAPHOS/SiO_2 gave the highest yield of the desired product, 50% at 65% conversion.

Reuse of catalyst was investigated for silica supported $[Rh(\mu-OCH_3)(C_8H_{12})]_2$ with (-)-DIOP. The yield of 1-hydroxy-1-phenylpropan-2-one at 70% conversion level remained in the range 23–25% when the catalyst was reused, although the final conversion level decreased from 95% to 76% in 5 h during catalyst recycling. This result indicates that Rh-(-)-DIOP/SiO_2 catalyst can be successfully reused in enantioselective hydrogenation of 1-phenyl-1,2-propanedione.

Table 4
Comparison of metal particle sizes and enantiomeric excesses in this work with literature data on PPD hydrogenation.

Catalyst	Metal particle size (nm)	Conditions	Conv. (%)	ee (%)	Ref.
5 wt% Pt/Al_2O_3	2.5	25 °C, 5 bar H_2, ethyl acetate, CD[a]	98	93	[29]
5 wt% Pt/SiO_2	3.7	25 °C, 5 bar H_2, ethyl acetate, CD[a]	98	64	[30]
Pt/SiO_2-CD, grafted CD	1.6	25 °C, 40 bar H_2, cyclohexane	97	41	[33]
1 wt % Rh-MCM-41-CD	3.2	25 °C, 20 bar H_2, cyclohexane	67	65	[63]
Rh-(R,R)-BDPP/SiO_2	4.8	25 °C, 40 bar H_2, cyclohexane	98	72	[19]
1 wt% Rh(-)-DIOP/SiO_2	1.7	25 °C, 40 bar H_2, cyclohexane	95	48	This work
1 wt% Pt/TNT-CD[b], grafted CD	1.7	25 °C, 40 bar H_2, cyclohexane	92	37	[35]
Pt(Pylm) /SiO_2	3.8	25 °C, 40 bar H_2, cyclohexane	65	48	[34]

[a] CD means added cinchonidine as a modifier.
[b] Titanate nanotubes.

Table 5
The results from recycling of Rh-(-)-DIOP/SiO_2 in PPD hydrogenation at 25 °C under 40 bar hydrogen. As a comparison the performance of Rh-(-)-DIOP nanoparticles is also presented here. Reaction conditions: PPD concentration 0.02 mol L^{-1}, (PPD/Rh) molar ratio: 100, 25 °C, 40 bar H_2, stirring rate: 800 rpm, solvent: 50 mL of cyclohexane. R-1 denotes *(R)*-1-hydroxy-1-phenylpropan-2-one.

Catalyst	GCLPA (%)	Conversion min (%) [a]	Yield of R-1 (%) [b]	ee_1 (%) [c]	ee_2 (%) [c]	rs [c]
Rh(-)-DIOP Nanoparticles	20	98	10	43	56	4
fresh Rh(-)-DIOP/SiO_2	23	95	23	40	40	5.5
once reused Rh(-)-DIOP/SiO_2	55	88	24	38	62	9
twice reused Rh(-)-DIOP/SiO_2	70	76	25	50	58	4

[a] after 240.
[b] 70% conversion.
[c] at 50% conversion.

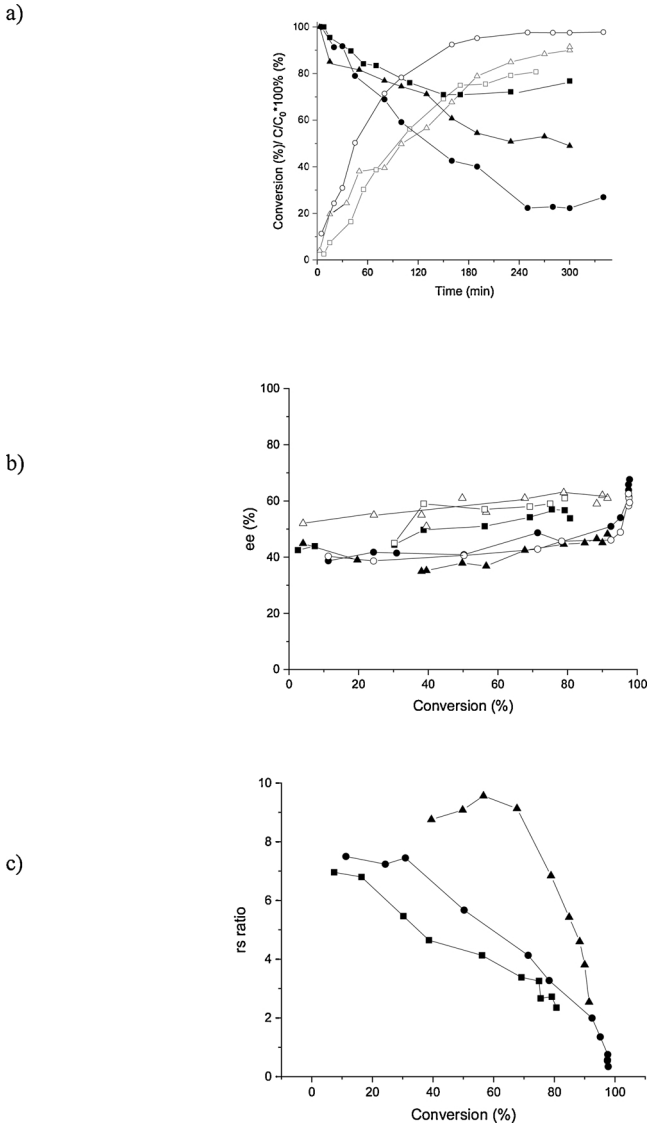

Fig. 11. a) Conversion (open symbol) and normalized total concentration of reactant (%, solid symbol) and products as a function of time, b) ee_1 (solid symbol) ee_2 (open symbol) and c) regioselectivity as a function of conversion in enantioselective hydrogenation of PPD over Rh-DIOP/SiO_2 at 25 °C under 40 bar in hydrogen. Symbols: fresh catalyst (●), reused once (▲) and reused twice (■), open symbol denotes conversion and closed symbol normalized total liquid phase concentration determined by GC.

Acknowledgements

Authors would like to acknowledge financial support of CONICYT through FONDECYT N° 1161660 project by financial support of this work. C. Claver and C. Godard are grateful to the Ministerio de Economia y Competividad and the Fondo Europeo de Desarrollo Regional FEDER (CTQ2016-75016-R, AEI/FEDER,UE).

References

[1] P.M. Subramanian, S.K. Chatterjee, M.C. Bhatia, Synthesis of (1RS, 2SR)-(±)-2-amino-1-phenyl-1-propanol from (R)-(−)-1-hydroxy-1-phenyl-2-propanone, J. Chem. Technol. Biot. 39 (4) (1987) 215–218.
[2] D. Gala, D.J. DiBenedetto, J.E. Clark, B.L. Murphy, D.P. Schumacher, M. Steinman, Preparations of antifungal Sch 42427/SM 9164: preparative chromatographic resolution, and total asymmetric synthesis via enzymatic preparation of chiral α-hydroxy arylketones, Tetrahedron Lett. 37 (5) (1996) 611–614.
[3] V.B. Shukla, P.R. Kulkarni, J. World, L-Phenylacetylcarbinol (L-PAC): biosynthesis and industrial applications, Microbiol. Biotechnol. 16 (2000) 499–506.
[4] Y. Orito, S. Imai, S. Niwa, Asymmetric hydrogenation of methyl pyruvate using Pt-C catalyst modified with cinchonidine, Nippon. Kagaku Kaishi 8 (1979) 1118–1120.
[5] Y. Orito, S. Imai, S. Niwa, G.H. Nguyen, Asymmetric hydrogenation of ethyl pyruvate on Pt/Al_2O_3 catalyst used cinchonidine as modifier, J. Synth. Org. Chem. Jpn. 37 (1979) 173–176.
[6] D.Yu. Murzin, P. Mäki-Arvela, E. Toukoniitty, T. Salmi, Asymmetric heterogeneous catalysis: science and engineering, Catal. Rev. Sci. Eng. 47 (2005) 175–256.
[7] P. Gallezot, D. Richard, Selective hydrogenation of α, β-unsaturated aldehydes, Catal. Rev. 40 (1-2) (1998) 81–126.
[8] G. Szöllősi, S.I. Niwa, T.A. Hanaoka, F. Mizukami, Enantioselective hydrogenation of α,β-unsaturated carboxylic acids over cinchonidine-modified Pd catalysts: effect of substrate structure on the adsorption mode, J. Mol. Catal. A Chem. 230 (1) (2005) 91–95.
[9] A. Roucoux, M. Devocelle, J.F. Carpentier, F. Agbossou, A. Mortreoux, Highly efficient asymmetric hydrogenation of activated and unactivated ketones catalyzed by Rhodium(I) aminophosphine and amidophosphine phosphinite complexes, Beneficial Effect of the Non Chiral Ligand, Synlett. 4 (1995) 358–360.
[10] J.L. Margitfalvi, E. Tálas, Enantioselective hydrogenation of ethyl pyruvate over cinchonidine–Pt/Al_2O_3 catalysts containing anchored silicium organic moieties, Appl. Catal. A Gen. 182 (1) (1999) 65–74.
[11] K. Borszeky, T. Mallat, A. Baiker, Enantioselective hydrogenation of α, β-unsaturated acids. Substrate-modifier interaction over cinchonidine modified $PdAl_2O_3$, Tetrahedron Asymmetry 8 (22) (1997) 3745–3753.
[12] D.J. Ager, A.H. Vries, J.G. Vries, Asymmetric homogeneous hydrogenations at scale, Chem. Soc. Rev. 41 (8) (2012) 3340–3380.
[13] Q.A. Chen, Z.S. Ye, Y. Duan, Y.G. Zhou, Homogeneous palladium-catalyzed asymmetric hydrogenation, Chem. Soc. Rev. 42 (2) (2013) 497–511.
[14] P. McMorn, G.J. Hutchings, Heterogeneous enantioselective catalysts: strategies for the immobilisation of homogeneous catalysts, Chem. Soc. Rev. 33 (2) (2004) 108–122.
[15] W. Tang, X. Zhang, New chiral phosphorus ligands for enantioselective hydrogenation, Chem. Rev. 103 (8) (2003) 3029–3070.
[16] A. Choplin, F. Quignard, From supported homogeneous catalysts to heterogeneous molecular catalysts, Coord. Chem. Rev. 178 (1998) 1679–1702.
[17] G. Szöllősi, A. Mastalir, Z. Kiraly, I. Dekany, Preparation of Pt nanoparticles in the presence of a chiral modifier and catalytic applications in chemoselective and asymmetric hydrogenations, J. Mater. Chem. 15 (25) (2005) 2464–2469.
[18] C. Mella, M. Avila, A. Sanchez, T. Marzialetti, P. Reyes, D. Ruiz, Chiral Rh/SiO_2 catalysts for enantioselective hydrogenation reactions: the role of (S,S)-DIPAMP as chiral modifier and stabilizer on metallic nanoparticles synthesis, J. Chil. Chem. Soc. 58 (4) (2013) 2125–2130.
[19] D. Ruiz, M. Oportus, C. Godard, C. Claver, J.L.G. Fierro, P. Reyes, Novel Metal

Nanoparticles Stabilized with (2R,4R)-2, 4-bis (diphenylphosphino)pentane on SiO_2. Their Use as Catalysts in Enantioselective Hydrogenation Reactions, Curr. Org. Chem. 16 (23) (2012) 2754–2762.
[20] R. Somanathan, N.A. Cortez, M. Parra-Hake, D. Chávez, G. Aguirre, Immobilized chiral metal catalysts for enantioselective hydrogenation of ketones, Mini. Org. Chem. 5 (4) (2008) 313–322.
[21] C. Bianchini, P. Barbaro, Recent aspects of asymmetric catalysis by immobilized chiral metal catalysts, Top. Catal. 19 (1) (2002) 17–32.
[22] E. Toukoniitty, P. Mäki-Arvela, N. Kumar, T. Salmi, D.Y. Murzin, Continuous enantioselective hydrogenation of ethyl benzoylformate over Pt/Al_2O_3 catalyst: bed dilution effects and cinchonidine adsorption study, Catal. Lett. 95 (2004) 179–183.
[23] E. Toukoniitty, P. Mäki-Arvela, M. Kuzma, D.Yu. Murzin, Enantioselective hydrogenation of 1-phenyl-1,2-propanedione, J. Catal. 204 (2001) 281–291.
[24] E. Toukoniitty, P. Mäki-Arvela, A.N. Villela, P.J. Kooyman, The effect of oxygen and the reduction temperature of the Pt/Al_2O_3 catalyst in enantioselective hydrogenation of 1-phenyl-1,2-propanedione, Catal. Today 60 (2000) 175–184.
[25] E. Toukoniitty, J. Wärnå, P. Mäki-Arvela, T. Salmi, D.Yu. Murzin, Application of transient methods in three-phase catalysis: hydrogenation of a dione in a catalytic plate column, Catal. Today 383 (2003) 79–80.
[26] E. Toukoniitty, P. Mäki-Arvela, A. Kalantar Neyestanaki, T. Salmi, D.Y. Murzin, Continuous hydrogenation of 1-phenyl-1,2-propanedione under transient and steady-state conditions: regioselectivity, enantioselectivity and catalyst deactivation, Appl. Catal. A Gen. 235 (2002) 125–138.
[27] E. Toukoniitty, P. Mäki-Arvela, N. Kumar, T. Salmi, D.Y. Murzin, Influence of mass transfer on regio- and enantioselectivity in hydrogenation of 1-phenyl-1,2-propanedione over modified Pt catalysts, Catal. Today 79–80 (2003) 189–193.
[28] E. Toukoniitty, P. Mäki-Arvela, V. Nieminen, M. Hotokka, J. Päivärinta, T. Salmi, D.Y. Murzin, Enhanced Regioselectivity in Batch and Continuous Hydrogenation of 1-phenyl-1,2-propanedione Over Modified Pt Catalysts, Catalysis of Organic Reactions, Marcel Dekker (Ed), New York, 2002, pp. 341–358.
[29] E. Toukoniitty, P. Mäki-Arvela, J. Wärnå, T. Salmi, Modeling of the enantioselective hydrogenation of 1-phenyl-1,2-propanedione over Pt/Al_2O_3, Catal. Today 66 (2–4) (2001) 411–417.
[30] E. Toukoniitty, P. Mäki-Arvela, A. Kalantar Neyestanaki, T. Salmi, R. Sjöholm, R. Leino, E. Laine, P. Kooyman, T. Ollonqvist, T. Väyrynen, Batchwise and continuous enantioselective hydrogenation of 1-phenyl-1,2-propanedione catalysed by new Pt/SiO_2 fibres, Appl. Catal. A Gen. 216 (2001) 73–83.
[31] C. Urbina, C. Campos, G. Pecchi, C. Claver, P. Reyes, Chiral Pt/ZrO_2 catalysts. Enantioselective hydrogenation of 1-phenyl-1,2-propanedione, Molecules 15 (2010) 3428–3440.
[32] D. Ruiz, C. Mella, J.L.G. Fierro, P. Reyes, Silica supported rhodium metal nanoparticles stabilized with (-)-DIOP. Effect of ligand concentration and metal loading on the enantioselective hydrogenation of ketones, J. Chil. Chem. Soc. 57 (4) (2012) 1394–1399.
[33] D. Ruiz, J.L.G. Fierro, P. Reyes, Enantioselective hydrogenation of ethyl pyruvate and 1-phenyl-1,2-propanedione on catalysts prepared by impregnation of colloidal platinum on SiO2, J. Braz. Chem. Soc. 21 (2) (2010) 262–269.
[34] C.H. Campos, C.C. Torres, A. Leyton, J. Belmar, C. Mella, P. Osorio-Vargas, D. Ruiz, J.L.G. Fierro, P. Reyes, A new non-cinchona chiral modifier immobilized on Pt/SiO_2 catalysts for enantioselective heterogeneous hydrogenation, Appl. Catal. A Gen. 498 (2015) 76–87.
[35] C.H. Campos, C.C. Torres, P. Osorio-Vargas, C. Mella, J. Belmar, D. Ruiz, J.L.G. Fierro, P. Reyes, Immobilized chiral inducer on Pt-based mesoporous titanate nanotubes as heterogeneous catalysts for enantioselective hydrogenation, J. Mol. Catal. A Chem. 398 (2015) 190–202.
[36] A. Lindholm, P. Mäki-Arvela, E. Toukoniitty, T. Salmi, D.Y. Murzin, R. Sjöholm, R. Leino, Hydrosilylation of cinchonidine and 9-O-TMS-cinchonidine with triethoxysilane: application of 11-(triethoxysilyl)-10,11-dihydrocinchonidine as a chiral modifier in the enantioselective hydrogenation of 1-phenyl-1,2-propanedione, Perkin Transactions I (2002) 2605–2612.
[37] Y. Huang, J. Chen, H. Chen, R. Li, Y. Li, L. Min, X. Li, Enantioselective hydrogenation of ethyl pyruvate catalyzed by PVP-stabilized rhodium nanoclusters, J. Mol. Catal. A Chem. 170 (2001) 143–146.
[38] V. Mévellec, A. Nowicki, A. Roucoux, C. Dujardin, P. Granger, E. Payen, K. Philippot, A simple and reproducible method for the synthesis of silica-supported rhodium nanoparticles and their investigation in the hydrogenation of aromatic compounds, New J. Chem. 30 (2006) 1214–1219.
[39] A. Roucoux, J. Schulz, H. Patin, Reduced Transition Metal Colloids. A Novel Family of Reusable Catalysts, Chem. Rev. 102 (2002) 3757–3778.
[40] H. Bönnemann, G.A. Braun, Enantioselective hydrogenations on platinum colloids, Angew. Chem. Int. Ed. Engl. 35 (17) (1996) 1992–1995.
[41] B. Chaudret, Organometallic approach to nanoparticles synthesis and self-organization, C. R. Phys. 6 (2005) 117–131.
[42] H. Bönnemann, G.A. Braun, Enantioselectivity control with metal colloids as catalyst, Eur. J. Clin. Chem. Clin. Biochem. 3 (1997) 1200–1202.
[43] P. Barbaro, V. Dal Santo, F. Liguori, Emerging strategies in sustainable fine-chemical synthesis: asymmetric catalysis by metal nanoparticles, Dalton Trans. 39 (36) (2010) 8391–8402.
[44] M.J. Jacinto, P.K. Kiyohara, S.H. Masunaga, R.F. Jardim, L.M. Rossi, Recoverable rhodium nanoparticles: synthesis, characterization and catalytic performance in hydrogenation reactions, Appl. Catal. A Gen. 338 (1) (2008) 52–57.
[45] J. Koktan, H. Sedláčková, I. Osante, C. Cativiela, D.D. Díaz, P. Řezanka, Chiral supramolecular nanoparticles: the study of chiral surface modification of silver nanoparticles by cysteine and its derivatives, Colloids Surf. A Physicochem. Eng. Asp. 470 (2015) 142–148.
[46] A. Roucoux, Stabilized Noble Metal Nanoparticles: an unavoidable family of catalysts for arene derivative hydrogenation, Top. Organomet. Chem. 16 (2005) 261–279.
[47] M. Axet, S. Castillón, C. Claver, K. Philippot, P. Lecante, B. Chaudret, Chiral diphosphite-modified Rhodium(0) nanoparticles: catalyst reservoir for styrene hydroformylation, Eur. J. Inorg. Chem. 22 (2008) 3460–3466.
[48] S. Jansat, M. Gomez, K. Philippot, G. Muller, E. Guiu, C. Claver, S. Castillon, B.A. Chaudret, Case for enantioselective allylic alkylation catalyzed by palladium nanoparticles, J. Am. Chem. Soc. 126 (2004) 1592–1593.
[49] S. Castillon, C. Claver, Y. Diaz, C1 and C2-symmetric carbohydrate phosphorus ligands in asymmetric catalysis, Chem. Soc. Rev. 34 (8) (2005) 702–713.
[50] H.J. Zhu, Y.J. Ding, L. Yan, J.M. Xiong, Y. Lu, L.W. Lin, The PPh 3 ligand modified Rh/SiO_2 catalyst for hydroformylation of olefins, Catal. Today 93 (2004) 389–393.
[51] E. Ramirez, S. Jansat, K. Philippot, P. Lecante, M. Gomez, A.M. Masdeu-Bultó, B. Chaudret, Influence of organic ligands on the stabilization of palladium nanoparticles, J. Organomet. Chem. 689 (24) (2004) 4601–4610.
[52] S.U. Son, Y. Jang, K.Y. Yoon, E. Kang, T. Hyeon, Facile synthesis of various phosphine-stabilized monodisperse palladium nanoparticles through the understanding of coordination chemistry of the nanoparticles, Nano Lett. 4 (6) (2004) 1147–1151.
[53] B. Léger, A. Denicourt-Nowicki, H. Olivier-Bourbigou, A. Roucoux, Rhodium nanocatalysts stabilized by various bipyridine ligands in nonaqueous ionic liquids: influence of the bipyridine coordination modes in arene catalytic hydrogenation, Inorg. Chem. 47 (19) (2008) 9090–9096.
[54] A. Gual, M.R. Axet, K. Philippot, B. Chaudret, A. Denicourt-Nowicki, A. Roucoux, S. Castillón, C. Claver, Diphosphite ligands derived from carbohydrates as stabilizers for ruthenium nanoparticles: promising catalytic systems in arene hydrogenation, Chem. Commun. (Camb.) (2008) 2759–2761.
[55] D. Han, X. Li, H. Zhang, Z. Liu, G. Hu, C. Li, Asymmetric hydroformylation of olefins catalyzed by rhodium nanoparticles chirally stabilized with (R)-BINAP ligand, J. Mol. Cat. A. Chem. 283 (2008) 15–22.
[56] A. Gual, C. Godard, K. Philippot, B. Chaudret, A. Denicourt-Nowicki, A. Roucoux, C. Claver, Carbohydrate-derived 1,3-diphosphite ligands as chiral nanoparticle stabilizers: promising catalytic systems for asymmetric hydrogenation, ChemSusChem. 2 (8) (2009) 769–779.
[57] C.W. Chen, T. Serizawa, M. Akashi, Preparation of platinum colloids on polystyrene nanospheres and their catalytic properties in hydrogenation, Chem. Mater. 11 (5) (1999) 1381–1389.
[58] A.B. Lowe, B.S. Sumerlin, M.S. Donovan, C.L. McCormick, Facile preparation of transition metal nanoparticles stabilized by well-defined (co) polymers synthesized via aqueous reversible addition-fragmentation chain transfer polymerization, J. Am. Chem. Soc. 124 (39) (2002) 11562–11563.
[59] S.A. Stratton, K.L. Luska, A. Moores, Rhodium nanoparticles stabilized with phosphine functionalized imidazolium ionic liquids as recyclable arene hydrogenation catalysts, Catal. Today 183 (1) (2012) 96–100.
[60] D. Han, X. Li, H. Zhang, Z. Liu, J. Li, C. Li, Heterogeneous asymmetric hydroformylation of olefins on chirally modified Rh/SiO_2 catalysts, J. Catal. 243 (2006) 318–328.
[61] M.L. Tschan, O. Diebolt, P.W.N.M. van Leeuwen, Ruthenium metal nanoparticles in hydrogenation: influence of phosphorus-ligands, Top. Catal. 57 (10-13) (2014) 1054–1065.
[62] T. Marzialetti, M. Oportus, D. Ruiz, J.L.G. Fierro, P. Reyes, Enantioselective hydrogenation of 1-phenyl-1,2-propanedione, ethyl pyruvate and acetophenone on Ir/SiO_2 catalysts: effect of iridium loading, Catal. Today 133 (2008) 711–719.
[63] C.C. Torres, C.H. Campos, J.L.G. Fierro, P. Reyes, D. Ruiz, Enantioselective hydrogenation of 1-phenyl-1,2-propanedione on cinchonidine-modified Rh/MCM-41 catalysts, J. Mol. Catal. A Chem. 392 (2014) 321–328.
[64] J. Chatt, L.M. Venanzi, Olefin coordination compounds. Diene complexes of rhodium(I), J. Chem. Soc. (1957) 4735–4741.
[65] R. Uson, L.A. Oro, J.A. Cabeza, Dinuclear methoxy, cyclooctadiene, and barrelene. Complexes of Rhodium(I) and Iridium(I), Inorg. Synth. 23 (1985) 126–130.
[66] V.B. Shukala, P.R. Kulkarni, L-phenylacetlcarbinol (L-PAC): biosynthesis and industrial applications, World J. Microbiol. Biotechnol. 16 (2000) 499–506.